Stochastic fluctuations and quasipattern formation in reaction-diffusion systems with anomalous transport

Joseph W. Baron[*] and Tobias Galla[†]

Theoretical Physics, School of Physics and Astronomy, The University of Manchester, Manchester M13 9PL, United Kingdom

Many approaches to modeling reaction-diffusion systems with anomalous transport rely on deterministic equations which ignore fluctuations arising due to finite particle numbers. Starting from an individual-based model we use a generating-functional approach to derive a Gaussian approximation for this intrinsic noise in subdiffusive systems. This results in corrections to the deterministic fractional reaction-diffusion equations. Using this analytical approach, we study the onset of noise-driven quasipatterns in reaction-subdiffusion systems. We find that subdiffusion can be conducive to the formation of both deterministic and stochastic patterns. Our analysis shows that the combination of subdiffusion and intrinsic stochasticity can reduce the threshold ratio of the effective diffusion coefficients required for pattern formation to a greater degree than either effect on its own.

I. INTRODUCTION

Reaction-diffusion schemes are a well-established tool for modeling nonlinear pattern-forming phenomena in a wide variety of systems, ranging from developmental biology [1–3] to chemical reactions [4], from the self-organization of slime mold [5] and the distribution of mussels [6] to Rayleigh-Bénard convection in fluids [7]. Most notably, Turing showed in his seminal work [8] that systems which have a stable fixed point when diffusion is not present could exhibit an instability in the presence of diffusion. He showed that diffusion, normally considered a stabilizing, equilibrating influence, combined with activator-inhibitor reaction dynamics, could provide a simple mechanism for pattern formation.

A difficulty that arises in the Turing interpretation of pattern formation is that the diffusion constants of the activator and inhibitor species are often required to be quite disparate for patterns to be found [9]. These large ratios of diffusion constants are unphysical.

One potential solution to this is that a system may not have to undergo a deterministic Turing instability to exhibit pattern formation. Stochastic quasipatterns, which arise due to the intrinsic noise of individual-based systems, may be sufficient to explain the spatial ordering observed in some natural systems [10,11]. The emergence of such quasipatterns requires a lower threshold ratio of diffusion coefficients than the emergence of deterministic patterns [12,13]. Noise-induced quasipatterns have been observed recently in experimental biological systems [14,15].

Another proposed solution to this problem is modeling one or more of the components as subdiffusing [16,17]; that is, diffusing with a mean-squared displacement which is sublinear in time. This has also been shown to reduce the ratio of the effective diffusion coefficients required for

pattern formation [18,19]. Furthermore, subdiffusion has been observed in many experimental systems with low particle numbers, such as proteins moving in the cell membrane [20,21] and in other transport phenomena involving obstacles or binding sites [22,23]. It has been argued that morphogens could be subject to similar binding and trapping effects and move subdiffusively as a result [24–26].

However, as of yet, the treatment of reaction-subdiffusion systems has been restricted to deterministic equations which ignore the stochastic effects due to the finite numbers of particles involved. Examples of the deterministic treatment include Refs. [25–27]. Stochastic effects due to demographic noise are important particularly in biological systems, where subdiffusion has been observed, and where the particle numbers involved can be sufficiently small for noise to be non-negligible. From a more theoretical perspective, subdiffusion is a non-Markovian phenomenon. Because of this, reaction-diffusion systems with subdiffusing components provide a good opportunity to study the combination of memory effects and intrinsic noise.

In this work, we use an individual-based approach, which explicitly takes into account intrinsic stochasticity, to study systems with reactions and anomalous diffusion. We carry out a path-integral (or generating-functional) analysis of the stochastic dynamics, combining transport and reactions, and perform an expansion in the strength of the intrinsic noise. To lowest order, effectively neglecting fluctuations, we recover the familiar deterministic reaction-subdiffusion equations. Taking into account subleading orders of fluctuations, we find additional coloured Gaussian noise terms in these equations, encapsulating the intrinsic stochasticity of the individual-based system. We show that the analytical expressions for this noise can be used to characterize the emergence of stochastic quasipatterns in reaction systems with subdiffusing components. Specifically, we use both the Brusselator [28] and Lengyel-Epstein [29,30] systems as examples. We conclude that the combination of the two effects, noise-driven quasipatterns and subdiffusion, can lower the critical ratio of diffusion

---

[*]joseph.baron@postgrad.manchester.ac.uk
[†]tobias.galla@manchester.ac.uk

coefficients required for pattern formation significantly, and to a greater degree than either effect on its own.

The remainder of this paper organized as follows: In Sec. II, we describe the individual-based model in detail and briefly present some background material related to subdiffusion and to the Brusselator and Lengyel-Epstein models. Section III contains an outline of our analysis of the individual-based system and the generating-functional approach to approximating the noise; further details of this calculation can be found in the Supplemental Material [31]. In Sec. IV, we show that this approach can be used to derive the familiar reaction-diffusion equations with fractional diffusion, now with additional noise terms. In Sec. V, we describe how one can then compute the fluctuations about the deterministic solution, using the linear-noise approximation. We verify our approach by comparing our theory predictions to stochastic simulations. In Sec. VI, we go on to use our theoretical approach to find the parameter regions where stochastic patterns are present and where deterministic patterns are present. Finally, in Sec. VII we discuss our results and conclude.

II. MODEL CONSTRUCTION AND BACKGROUND

In this section we introduce our model and the general notation, and we briefly summarize some background material. We also define the Brusselator and Lengyel-Epstein reaction schemes, which we later use to illustrate the formation of quasipatterns in stochastic subdiffusive systems.

A. Individual-based model

We consider a general class of individual-based reaction-diffusion models. We refer to the individuals as "particles" from here on, but these particles may represent biological entities or molecules of chemical reactants.

Several species of particle react with one another and hop around on a discrete lattice. We use α to index the different species. Each lattice site can be occupied by multiple particles simultaneously, and we denote the number of particles of type α at site i at time t by $n_{i,t}^{\alpha}$. Reactions between particles occur locally within a given site of the lattice and result in the annihilation and creation of particles or the conversion of one type of particle into another. For the purposes of simplicity, we will confine ourselves to a discrete one-dimensional lattice with periodic boundary conditions. Most of our analysis could be generalized to other spatial arrangements or to higher dimensions, and indeed the continuum limit may be taken.

Particles are assigned a random waiting-time at birth (creation), drawn from an as yet unspecified waiting-time probability density function $\psi^{\alpha}(\tau)$. This may be different for the different species of particle, as indicated by the superscript. The particle then hops to a new location once it has waited for the assigned time, assuming that it has not been eliminated in a reaction. A new waiting-time is drawn from $\psi^{\alpha}(\tau)$ once the particle has hopped and the process begins again. This means that a particle which has been at its current site for an amount of time τ hops with a rate $h_{\tau}^{\alpha} = \frac{\psi^{\alpha}(\tau)}{\Psi^{\alpha}(\tau)}$, where $\Psi^{\alpha}(\tau) = 1 - \int_0^{\tau} \psi^{\alpha}(\tau')d\tau'$ is the survival probability. The quantity h_{τ}^{α} is often referred to as the hazard rate [16]; we use subscript notation for τ for later convenience. When the

particle does hop, its new location is drawn from the hopping kernel $\phi_{i,i'}$. Here $\phi_{i,i'}$ is the probability that the particle hops from location i' to i, given that a hopping event occurs. For our purposes, $\phi_{i,i'}$ will be a function of $|i' - i|$ only, so as to ensure the translational invariance of the problem. In principle the hopping kernel could also be different for the different species. To keep the model simple we use the same hopping kernel for all species; it is straightforward to extend the model to the more general case.

During the particles' sojourn periods at a given site, they may undergo reactions. We index the various reaction types with r. The rate $\lambda_{i,r,t}$ at which reactions of type r occur at site i is in general dependent on the number of particles of the various types currently at site i. We denote the number of particles of type α that are produced or annihilated in a reaction of type r by ν_r^{α}, which can be positive or negative. The constants ν_r^{α} are the so-called stoichiometric coefficients [32]. If a particle is annihilated in a reaction, then the hop which was scheduled to occur for that particle no longer occurs. As a result of this and of the fact that the reaction rates depend on local concentrations, the hopping process and the reactions are interdependent and cannot easily be separated as in conventional reaction-diffusion equations (such as those used by Turing [8]).

B. Subdiffusion

We first discuss the phenomenon of subdiffusion in the case where particles undergo hopping events but no reactions. Particles are said to undergo subdiffusion if the mean-squared displacement for a single particle behaves as follows in the long term: $\langle x(t)^2 \rangle \sim t^{\gamma}$, where $0 < \gamma < 1$. The behavior approaches normal diffusion as $\gamma \to 1$. Subdiffusive transport may be produced by choosing a long-tailed waiting-time distribution $\psi(t)$ for particles which hop around as described in the previous section (for the time being we suppress the dependence on the particle species α). The distribution we will use in this paper to model subdiffusion is that of Mittag-Leffler, which produces the desired behavior and is particularly convenient for the theoretical analysis. That is, we choose $\psi(t) = -\frac{d}{dt}E_{\gamma}[-(\frac{t}{t_0})^{\gamma}]$ where $E_{\gamma}[x]$ is the Mittag-Leffler function [33]. The parameter t_0 sets the overall scale of the hopping process. This distribution has the convenient property that its Laplace transform is given by $\hat{\psi}(u) = \frac{1}{1+(t_0 u)^{\gamma}}$. Notably, for $\gamma = 1$ the Mittag-Leffler function reduces to an exponential such that $\psi(t) = \frac{1}{t_0}e^{-\frac{t}{t_0}}$.

For a single species of diffusing particle, which undergoes no reactions, one may use the Mittag-Leffler waiting-time distribution, along with the Montroll-Weiss formula [34,35], to recover the fractional diffusion equation [16,36,37],

$$\frac{\partial P_{i,t}}{\partial t} = \sum_{i'}(\phi_{i,i'} - \delta_{i,i'})t_0^{-\gamma} {}_0D_t^{1-\gamma}P_{i,t}, \qquad (1)$$

where $P_{i,t}$ is the probability of finding a particular particle at position i at time t. The Riemann-Liouville fractional derivative ${}_0D_t^{1-\gamma}$ is defined as

$${}_0D_t^{1-\gamma}f(t) = \frac{1}{\Gamma(\gamma)}\frac{\partial}{\partial t}\int_0^t \frac{f(t')}{(t - t')^{1-\gamma}}dt', \qquad (2)$$

where $\Gamma(\cdot)$ denotes the gamma function. The fractional derivative has the property

$$\mathcal{L}_t\{_0D_t^{1-\gamma}f(t)\}(u) = u^{1-\gamma}\hat{f}(u), \qquad (3)$$

where we use $\mathcal{L}_t$ to denote the Laplace transform with respect to t. One can show from Eq. (1) that $\langle i^2 \rangle = \frac{2}{3\Gamma(1+\gamma)}(\frac{t}{t_0})^\gamma$, if one uses the symmetrical hopping kernel
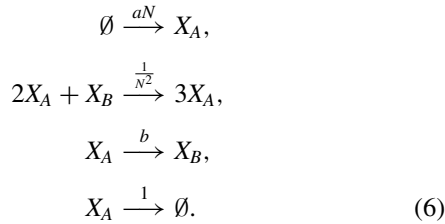
$$\phi_{i,i'} = \begin{cases} \frac{1}{3}, & \text{if } i = i' + 1 \\ \frac{1}{3}, & \text{if } i = i' \\ \frac{1}{3}, & \text{if } i = i' - 1 \end{cases}. \qquad (4)$$

In our system, different species of particles may hop with different typical waiting times t_0^α and different anomalous exponents γ^α. Precisely, the waiting-time distributions for each species are given by

$$\psi^\alpha(t) = -\frac{d}{dt}\left\{E_{\gamma^\alpha}\left[-\left(\frac{t}{t_0^\alpha}\right)^{\gamma^\alpha}\right]\right\}. \qquad (5)$$

C. Reaction schemes

As example systems, we will use the Brusselator [28] and the Lengyel-Epstein [29,30] models. The Brusselator is an activator-inhibitor model, first conceived of to describe oscillatory chemical reactions such as the Belousov-Zhabotinsky reaction [38]. The reactions between the two species of particle involved, A and B, are given by

$$\emptyset \xrightarrow{aN} X_A,$$

$$2X_A + X_B \xrightarrow{\frac{1}{N^2}} 3X_A,$$

$$X_A \xrightarrow{b} X_B,$$

$$X_A \xrightarrow{1} \emptyset. \qquad (6)$$

Without hopping the system has a homogeneous stable deterministic fixed point at $\bar{n}^{(A)} = aN$, $\bar{n}^{(B)} = \frac{b}{a}N$ so long as $b < 1 + a^2$, where $\bar{n}^{(\alpha)}$ is the number of particles of type α at the fixed point.

The Lengyel-Epstein model was introduced primarily as a way of modeling the ClO$_2^-$-I$^-$-MA reaction, which exhibits Turing patterns experimentally [39]. We use a simplified two-species version of the full model, which effectively assumes that the concentrations of the remaining components are constant. The reactions are given by

$$\emptyset \xrightarrow{aN} X_A,$$

$$X_A \xrightarrow{b} X_B,$$

$$4X_A + X_B \xrightarrow{R} \emptyset, \qquad (7)$$
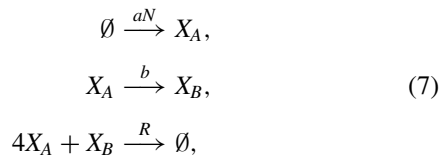
where the rate $R = \frac{1}{(n^{(A)})^3}\frac{cN}{dN^2+(n^{(A)})^2}$ is dependent on the concentration of type-A particles. The Lengyel-Epstein system has a homogeneous deterministic fixed point at $\bar{n}^{(A)} = \frac{aN}{5b}$, $\bar{n}^{(B)} = \frac{bdN}{c}[1 + (\frac{\bar{n}^{(A)}}{\sqrt{dN}})^2]$ so long as $ca > \frac{3}{5}a^2 - 25b^2d$.

In both models, species A is the activator and species B is the inhibitor. The parameter N in both systems characterizes the typical number of particles per site and will become

useful to us later when we perform a system-size expansion to analyze noise in the these systems. The reaction rates (the number of reactions which occur per unit time) are calculated according to the usual mass action kinetics [40]. For example, the rate at which the last reaction in Eq. (7) occurs is $R \times (n^{(A)})^4 \times n^{(B)} = \frac{cNn^{(A)}n^{(B)}}{dN^2+(n^{(A)})^2}$.

III. APPROXIMATION OF THE FLUCTUATIONS IN PARTICLE NUMBER USING GAUSSIAN NOISE

A. Formulation of the problem

To capture the noise-driven effects in the models described in Sec. II A, we carry out an expansion in the inverse system-size. The idea is similar to the principles underlying the Kramers–Moyal expansion or the system-size expansion by van Kampen for Markovian systems [41]. However, there are also conceptual differences due to the non-Markovian nature of subdiffusion.

To carry out the expansion, we use the reciprocal of the parameter N in Eqs. (6) and (7); N characterizes the typical particle number per site. More specifically, ensemble-averaged particle numbers are of the order N at each lattice site, whereas the fluctuations in particle numbers are of the order $\sqrt{N}$. Thus, for large N, the noise is small in relative terms. The limit $N \to \infty$ reproduces the deterministic behavior, and when N is large but finite the expansion can be expected to accurately describe stochastic corrections. By performing the expansion, we obtain a set of stochastic differential equations (SDEs) [42] with Gaussian noise terms. These SDEs encapsulate not only the deterministic trajectory of the system but also the next-order stochastic noise corrections.

A complicating feature of systems where the waiting-time distribution for the hops is nonexponential is that the hazard rate for hopping is nonconstant, meaning that what happens at a given point in time is dependent on the history of the system. A sensible and common way to deconvolute the problem is to introduce the age coordinate τ, which denotes the length of time that a particle has resided at a particular location since its last hop [43]. That is, we denote the number of particles of type α which have resided at site i for a time between τ_1 and τ_2 by $\int_{t_1}^{t_2} n_{i,\tau,t}^\alpha d\tau$. This effectively recasts the problem as Markovian. The quantity $n_{i,\tau,t}^\alpha$ is a density of particles per time τ.

To develop the formalism we discretize time into steps of size Δ. We assume that all reaction rates and hopping rates remain constant during each step, similar to the τ-leaping approach to Gillespie simulations in discrete time [44]. Eventually, we will take the limit $\Delta \to 0$ to restore continuous time.

For our system, the quantity $n_{i,\tau,t}^\alpha$ may change due to two effects in each time step: reactions and hopping. We represent the changes due to these effects by the following quantities, respectively: $k_{i,r,\tau,t}^{(R)\alpha}$ and $k_{i,i',\tau,t}^{(H)\alpha}$. That is, $k_{i,r,\tau,t}^{(R)\alpha}$ is the number of particles of type α and age τ at position i which are annihilated in the time step from t to $t + \Delta$ due to reactions of type r. We note that newly created particles have age zero; this will be dealt with separately below. Similarly, $k_{i,i',\tau,t}^{(H)\alpha}$ is the number of particles of age τ hopping away from position i' to i at time t. The sets of integer variables $\{k_{i,r,\tau,t}^{(R)\alpha}\}$ and

$\{k_{i,i',\tau,t}^{(H)\alpha}\}$ are stochastic, that is they take different values for every realization of the system.

We then have

$$n_{i,\tau+\Delta,t+\Delta}^{\alpha} - n_{i,\tau,t}^{\alpha} = -\sum_r \frac{k_{i,r,\tau,t}^{(R)\alpha}\theta(-\nu_r^\alpha)}{\Delta} - \sum_{i'} \frac{k_{i',i,\tau,t}^{(H)\alpha}}{\Delta},$$

(8)

where $\theta(\cdot)$ denotes the Heaviside function. We note that, in the discrete-time setup, the total number of particles at site i at time t is given by $n_{i,t}^\alpha = \Delta \sum_m n_{i,\tau=m\Delta,t}^\alpha$; the quantity $n_{i,\tau,t}^\alpha$ therefore has dimensions of inverse time, in-line with the expression on the right-hand side of Eq. (8).

Equation (8) only includes reactions which annihilate particles, i.e., it describes the outflux of particles from position i. When particles are produced, or when they newly arrive at a location after hopping, they have age $\tau = 0$. Therefore, the influx of particles to position i is given by

$$n_{i,0,t+\Delta}^\alpha = \sum_r \frac{\ell_{i,r,t}^{(R)} \nu_r^\alpha \theta(\nu_r^\alpha)}{\Delta} + \sum_{i'} \frac{k_{i,i',\tau,t}^{(H)\alpha}}{\Delta},$$

(9)

where $\ell_{i,r,t}^{(R)}$ is the number of reactions of type r firing in the time window t to $t+\Delta$ at position i. We note also that $\theta(-\nu_r^\alpha)\ell_{i,r,t}^{(R)}|\nu_r^\alpha| = \sum_\tau k_{i,r,\tau,t}^{(R)\alpha}$. Furthermore, particles of a given species which are annihilated due to a reaction at a given site are selected at random from all particles of this species at the site, irrespective of age.

B. Generating functional approach to the system-size expansion

To approximate the stochastic fluctuations in particle number with Gaussian noise, one would normally write down a master equation and expand in powers of N^{-1} to obtain a Fokker-Planck equation; see, for example, Refs. [13,42,45,46]. From this Fokker-Planck equation one could read off the corresponding SDE. Since the hopping of the particles in our system is history-dependent, there is no straightforward way to write down a master equation, even after the introduction of the additional age coordinate τ. The most natural way to analyze a non-Markovian stochastic system is with the Martin-Siggia-Rose-Janssen-De Dominicis (MSRJD) path integral, which takes into account all possible histories of the system [47–49]. Such an approach allows one to perform the expansion in inverse powers of the system-size without writing down a master equation explicitly [50,51].

To reflect the system-size dependence in our calculation we introduce $x_{i,\tau,t}^\alpha = \frac{n_{i,\tau,t}^\alpha}{N}$. These quantities are of order N^0. The MSRJD generating functional then takes the form of a path integral over all possible trajectories of the variables $\{x_{i,\tau,t}^\alpha\}$ [52]. It can be written as

$$Z[\{\Xi_{i,\tau,t}^\alpha\}] = \left\langle \exp\left(i \sum_{i,\alpha,\tau,t} \Xi_{i,\tau,t}^\alpha x_{i,\tau,t}^\alpha\right) \right\rangle_{\{x_{i,\tau,t}^\alpha\}},$$

(10)

where $\langle \dots \rangle_{\{x_{i,\tau,t}^\alpha\}}$ denotes an average over all trajectories of the system. The $\{\Xi_{i,\tau,t}^\alpha\}$ are source variables. The procedure for performing the expansion in N^{-1} is similar to that used

in Refs. [50,51]: We find the joint probability distribution for the sets of variables $\{k_{i,r,\tau,t}^{(R)\alpha}\}$ and $\{k_{i,i',\tau,t}^{(H)\alpha}\}$ and rewrite the generating functional in term of these quantities. We then average these random numbers against their joint distribution, to obtain the generating functional in terms of only the coordinates $\{x_{i,\tau,t}^\alpha\}$ and the model parameters. We then carry out an expansion in N^{-1} up to and including subleading order. This approximate generating functional is recognized as that of an effective SDE. The leading-order terms in this SDE correspond to the deterministic dynamics; after further rearrangement it reproduces the well-known deterministic reaction-subdiffusion equation, as shown in Sec. IV. This deterministic approximation is accurate in the limit $N \to \infty$. The next-order terms correspond to Gaussian noise corrections, with a standard deviation of order $N^{-1/2}$.

The details of this procedure are provided in the Supplemental Material (Secs. S1 and S2 [31]); here we only quote the final result, in which we have restored continuous time. It is given by the following stochastic equations:

$$\frac{\partial n_{i,\tau,t}^\alpha}{\partial t} + \frac{\partial n_{i,\tau,t}^\alpha}{\partial \tau} = -h_\tau^\alpha n_{i,\tau,t}^\alpha - p_{i,t}^\alpha n_{i,\tau,t}^\alpha + \xi_{i,\tau,t}^\alpha,$$

$$n_{i,0,t}^\alpha = \sum_{i'} \phi_{i,i'} \int_0^t h_\tau^\alpha n_{i',\tau,t}^\alpha d\tau + \gamma_{i,t}^\alpha + \xi_{i,0,t}^\alpha.$$

(11)

In these expressions, $p_{i,t}^\alpha$ is the per capita removal rate for particles of species α at position i and time t; $\gamma_{i,t}^\alpha$ is the total production rate for the particles of type α at i and t, that is

$$p_{i,t}^\alpha n_{i,\tau,t}^\alpha = \sum_r \lambda_{i,r,t} |\nu_r^\alpha| \frac{n_{i,\tau,t}^\alpha}{n_{i,t}^\alpha} \theta(-\nu_r^\alpha),$$

$$\gamma_{i,t}^\alpha = \sum_r \lambda_{i,r,t} |\nu_r^\alpha| \theta(\nu_r^\alpha).$$

(12)

The quantities $\lambda_{i,r,t}$, ν_r^α, $\phi_{i,i'}$, and h_τ^α are defined in Sec. II A. The fraction $n_{i,\tau,t}^\alpha/n_{i,t}^\alpha$ in the first of the relations in Eq. (12) reflects the fact that the particles which are to be removed are selected irrespective of their age τ. The quantities $\{\xi_{i,\tau,t}^\alpha\}$ in Eq. (11) represent white Gaussian noise of zero mean. Eqs. (11) are approximations of the full random process given by Eqs. (8) and (9), in which the randomness is discrete. While the noise $\{\xi_{i,\tau,t}^\alpha\}$ is white, we note that the components are correlated across species and lattice sites. The expressions for these correlations are somewhat lengthy; we derive and give them in Sec. S2 of the Supplemental Material [31]. It is also important to note that the noise is multiplicative, i.e., the elements in the covariance matrix of the $\{\xi_{i,\tau,t}^\alpha\}$ depend on the variables $\{n_{i,\tau,t}^\alpha\}$. This is similar to the outcome of a Kramers–Moyal expansion of the master equation for conventional Markovian systems [42,45].

IV. FRACTIONAL REACTION-DIFFUSION EQUATION WITH NOISE

Using the waiting-time distributions discussed in Sec. II B in conjunction with Eqs. (11), we are able to obtain the fractional reaction-diffusion equation reported in the literature (see, e.g., Refs. [18,25,26,53]) if we neglect the noise terms.

Including these terms, we are able to capture effects driven by the stochasticity of the original individual-based dynamics.

One proceeds from Eqs. (11) by integrating out the age variables τ, with the aim of finding a time-evolution equation in terms of only $n_{i,t}^{\alpha}$ and the noise. Using the Mittag-Leffler function from Eq. (5) as the waiting-time distribution, one arrives at the following fractional reaction-diffusion equation for the particle number $n_{i,t}^{\alpha}$:

$$\frac{\partial n_{i,t}^{\alpha}}{\partial t} = \sum_{i'} \left\{ (\phi_{i,i'} - \delta_{i,i'})(t_0^{\alpha})^{-\gamma^{\alpha}} e^{-\int_0^t p_{i',T'}^{\alpha} dT'} {}_0 D_t^{1-\gamma^{\alpha}} \left[n_{i',t}^{\alpha} e^{\int_0^t p_{i',T'}^{\alpha} dT'} \right] \right\} + f_{i,t}^{\alpha} + \eta_{i,t}^{\alpha}, \tag{13}$$

where we have defined the total reaction rate $f_{i,t}^{\alpha} = \gamma_{i,t}^{\alpha} - p_{i,t}^{\alpha} n_{i,t}^{\alpha}$.

In the limit of continuous space, the sum involving the hopping kernel becomes a Laplacian operator (i.e., $\sum_{i'} (\phi_{i,i'} - \delta_{i,i'}) \rightarrow \sigma^2 \nabla^2$, with a suitable constant σ^2, related to the variance of hopping distances). Thus, the fractional reaction-diffusion equation Eq. (13) corresponds to Eq. (3) in Ref. [18], but with the addition of a noise term. We recover the deterministic reaction-subdiffusion equation if we take the infinite system-size limit, $N \rightarrow \infty$, whereupon the noise becomes negligible.

One notes that the reaction and diffusion terms in Eq. (13) are coupled. This is due to the non-Markovian nature of the hopping and the fact that particles may be annihilated in reactions and are thus unable to perform scheduled hops. The exponential factors in Eqs. (13) correspond to the probability of particles surviving without being annihilated in a reaction.

The noise also involves such exponential factors and is given by

$$\eta_{i,t}^{\alpha} = \sum_{i'} \left\{ (\phi_{i,i'} - \delta_{i,i'}) \left[\int_0^t \psi^{\alpha}(\tau) e^{-\int_{t-\tau}^t p_{i',T'}^{\alpha} dT'} \int_0^{\tau} \frac{\xi_{i',T,T+t-\tau}^{\alpha}}{\Psi^{\alpha}(T) e^{-\int_0^T p_{i',T'+t-\tau}^{\alpha} dT'}} dT d\tau \right. \right.$$

$$\left. \left. - e^{\int_0^t p_{i',T'}^{\alpha} dT'}(t_0^{\alpha})^{-\gamma^{\alpha}} {}_0 D_t^{1-\gamma^{\alpha}} \left(\int_0^t \Psi^{\alpha}(\tau) e^{\int_0^{t-\tau} p_{i',T'}^{\alpha} dT'} \int_0^{\tau} \frac{\xi_{i',T,T+t-\tau}^{\alpha}}{\Psi^{\alpha}(T) e^{-\int_0^T p_{i',T'+t-\tau}^{\alpha} dT'}} dT d\tau \right) \right] \right\}$$

$$+ \int_0^t \xi_{i,\tau,t}^{\alpha} d\tau + \xi_{i,0,t}^{\alpha} . \tag{14}$$

The derivation of Eqs. (13) and (14) from Eqs. (11) broadly follows the method in Ref. [53] or Ref. [54] but also handles the additional noise terms. It is given in the Supplemental Material ([31] Sec. S3). The noise variables $\{\eta_{i,t}^{\alpha}\}$ involve integrals of the $\{\xi_{i,\tau,t}^{\alpha}\}$ and as a consequence they are correlated in time in addition to their correlations across components and lattice sites. Given that the statistics of $\{\xi_{i,\tau,t}^{\alpha}\}$ depend on the variables $\{n_{i,\tau,t}^{\alpha}\}$, this noise is multiplicative as well.

Although the expression for the noise $\eta_{i,t}^{\alpha}$ in Eq. (14) appears cumbersome at first glance, a great deal of simplification can be achieved in the regime where one considers small deviations about the homogeneous fixed point of the deterministic system. We discuss this in the next section.

One notes that for $\gamma \rightarrow 1$ we recover the normal reaction-diffusion equation where the reactions and diffusion are uncoupled:

$$\frac{\partial n_{i,t}^{\alpha}}{\partial t} = \sum_{i'} \left[(\phi_{i,i'} - \delta_{i,i'})(t_0^{\alpha})^{-1} n_{i',t}^{\alpha} \right] + f_{i,t}^{\alpha} + \eta_{i,t}^{\alpha}. \tag{15}$$

In this case, the expression for the noise also simplifies greatly and contains no exponential factors:

$$\eta_{i,t}^{\alpha} = \int_0^t \xi_{i,\tau,t}^{\alpha} d\tau + \xi_{i,0,t}^{\alpha}. \tag{16}$$

This can be seen from Eq. (14) by using the fact that the Mittag-Leffler function reduces to an exponential in the limit $\gamma \rightarrow 1$ and that the fractional derivative becomes an identity operator. In this special case, $\langle \xi_{i,\tau,t}^{\alpha} \xi_{i',\tau',t'}^{\alpha} \rangle \propto \delta(t - t')$, and we then also have $\langle \eta_{i,\tau,t}^{\alpha} \eta_{i',\tau',t'}^{\alpha} \rangle \propto \delta(t - t')$. Therefore, in the Markovian limit, we recover white noise. This is explored further in the Supplemental Material ([31] Sec. S2).

V. LINEAR-NOISE APPROXIMATION AND COMPARISON WITH SIMULATIONS

A. Linear-noise approximation

We now derive explicit expressions for the deviations of the stochastic system (i.e., with a finite number of particles per lattice site) from the solution of the deterministic reaction-subdiffusion equation.

We write $\bar{n}_{i,t}^{\alpha}$ for the solution of Eq. (13) with the noise term removed, and define the deviation from this deterministic solution through

$$n_{i,t}^{\alpha} = \bar{n}_{i,t}^{\alpha} + \delta_{i,t}^{\alpha}. \tag{17}$$

We focus on fluctuations about the steady state, i.e., we assume that $\bar{n}_{i,t}^{\alpha} \equiv \bar{n}^{\alpha}$ is the homogeneous fixed point of the deterministic system. From the results stated so far, we are able to compute the correlation matrix of the fluctuations $\langle \delta_{i,t}^{\alpha} \delta_{i',t'}^{\alpha'} \rangle$, which we then compare with results from stochastic simulations of the individual-based system.

The expansion in powers of N^{-1} in Sec. III was based on the assumption that the fluctuations about the deterministic trajectory were small in comparison to the total numbers of particles. A more precise formulation of this assumption allows us to make further simplifications. Since the noise term $\eta_{i,t}^{\alpha}$ in Eq. (13) is of order $N^{1/2}$, it is also reasonable that the fluctuations would be such that $\delta_{i,t}^{\alpha} \sim \mathcal{O}(N^{1/2})$. This is similar to the assumption used by van Kampen [41] to perform the system-size expansion now named after him. Using this, one can expand Eq. (13) about the deterministic fixed point $\bar{n}^{\alpha}$.
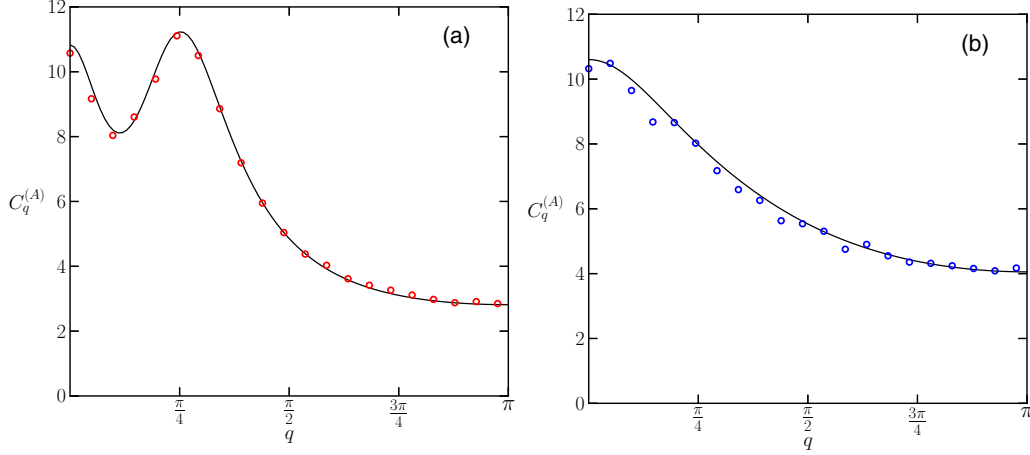
FIG. 1. The correlator $C_q^{(A)} = \langle |\tilde{\delta}_{q,t}^{(A)}|^2 \rangle / N$ for the Brusselator model with a subdiffusing activator (a) and a subdiffusing inhibitor (b). The markers represent simulation results and the solid lines depict results derived from the theory in the text. The model parameters are (a) $t_0^{(A)} = 0.6$, $t_0^{(B)} = 0.1$, and (b) $t_0^{(A)} = 1.33$, $t_0^{(B)} = 0.1$, giving an effective diffusion coefficient ratio of $\theta_\gamma = 4.63$ for both plots [see Eqs. (19) and (20)]. The remaining model parameters are $N = 4000$, $b = 1.8$, and $a = 1.1$. We have $\gamma = 0.5$ for the subdiffusing component in both figures. One observes that a range of nonzero Fourier modes q are excited to a greater extent than the $q = 0$ mode when the activator is subdiffusing (a) for this parameter set. This is not the case when inhibitor subdiffuses (b). The simulations were averaged over 1000 trials with 41 discrete positions on the lattice. Data was taken at $t = 20$ to ensure a stationary state had been reached.

We note that the $\delta_{i,t}^\alpha$ are small deviations about the homogeneous deterministic fixed point. The correlators $\langle \delta_{i,t}^\alpha \delta_{i',t'}^{\alpha'} \rangle$ therefore do not describe any deterministic pattern-forming features of the system. Instead, they characterize stochastic phenomena induced by fluctuations due to finite system sizes N.

To leading order (i.e., sending $N \to \infty$) we obtain the deterministic dynamics already mentioned, and in which all noise terms are removed. The terms to subleading order result in a linear expression for the fluctuations $\delta_{i,t}^\alpha$ in terms of $\eta_{i,t}^\alpha$. Within this order of approximation the quantities dependent upon $n_{i,t}^\alpha$ in the noise correlators $\langle \eta_{i,t}^\alpha \eta_{i',t'}^\alpha \rangle$ are evaluated at the fixed point $\bar{n}^\alpha$. The noise in the dynamics for the $\{\delta_{i,t}^\alpha\}$ is therefore now additive rather than multiplicative. The procedure is discussed further in Sec. S4 of the Supplemental Material [31].

Once the linearized equations are found, the problem is most naturally handled by taking Fourier and Laplace transforms with respect to the spatial and temporal coordinates, respectively. We use $\mathcal{F}_n\{f_n\}(q) = \sum_n e^{inq} f_n = \tilde{f}_q$ to denote the discrete Fourier transform and $\mathcal{L}_t\{g_t\}(u) = \int_0^t e^{-ut} g(t) dt = \hat{g}_u$ to denote the Laplace transform. We then obtain equations of the form

$$\hat{\tilde{\underline{\delta}}}_{u,q} = \hat{\underline{\underline{\tilde{m}}}}_{u,q} \hat{\tilde{\underline{\epsilon}}}_{u,q}, \tag{18}$$

with suitable Gaussian noise variables $\{\hat{\tilde{\epsilon}}_{u,q}^\alpha\}$. In the time domain this noise is colored. We use underscores to indicate vectors in the space of species. The square matrix $\hat{\underline{\underline{\tilde{m}}}}_{u,q} = (\hat{\tilde{m}}_{u,q})^{\alpha\beta}$ has dimension equal to the number of particle species. Its precise form is given in the Supplemental Material ([31] Sec. S4), as are full expressions for the correlators $\langle \tilde{\epsilon}_{q,t}^\alpha \tilde{\epsilon}_{q',t'}^{\alpha'} \rangle$.

It then remains to invert the Fourier and Laplace transforms. Expressions for the resulting correlators $\langle \delta_{i,t}^\alpha \delta_{i',t'}^{\alpha'} \rangle$ are given in the Supplemental Material ([31] Sec. S5). In practice,

the evaluation of the correlators $\langle \delta_{i,t}^\alpha \delta_{i',t'}^{\alpha'} \rangle$ is performed using numerical inverse Laplace transform methods (such as that of Zakian [55]) and fast Fourier transform routines. This is because analytical expressions for the inverse transforms of the elements of $\hat{\underline{\underline{\tilde{m}}}}_{u,q}$ are in general difficult to find. That being said, the equal-time equal-wave-number correlator, $\langle \tilde{\delta}_{q,t}^{(\alpha)} \tilde{\delta}_{q,t}^{(\alpha')\star} \rangle$, can indeed be found without the use of a numerical inverse Laplace transform technique (see Sec. S5 of the Supplemental Material [31]).

B. Comparison of theory to simulation results

The theory hitherto presented can be expected to be accurate when fluctuations about the deterministic homogeneous fixed point are small enough so that the linear approximation is valid. The examples in Figs. 1 and 2 show that one obtains good agreement with individual-based simulations of the full system with typical particle numbers per lattice site as low as $N \approx 4000$.

Figure 1 demonstrates the accuracy of the theory for the steady-state power-spectrum of fluctuations $\langle |\tilde{\delta}_{q,t}^{(A)}|^2 \rangle$ for the case of the Brusselator model. We compare the results of simulations to our theory for the cases where the activator subdiffuses and the inhibitor diffuses normally, and vice versa. Figure 2 again compares the theory predictions to Monte Carlo simulations but this time in the case of the Lengyel-Epstein model with a subdiffusing activator and a subdiffusing inhibitor. The autocorrelators $\langle \delta_{i,t}^{(A)} \delta_{i',t'}^{(A)} \rangle$ and $\langle \delta_{i,t}^{(B)} \delta_{i',t'}^{(B)} \rangle$ and the crosscorrelator $\langle \delta_{i,t}^{(A)} \delta_{i',t'}^{(B)} \rangle$ are shown for different temporal separations $t - t'$ and spatial separations $i - i'$. The agreement in both Figs. 1 and 2 is good apart from some minor deviations. These arise from a combination of the stochastic nature of the simulations and the limits to the accuracy of the numerical inverse Laplace transform. The discrepancy reduces as the number of trials, over which the average is taken, is increased.
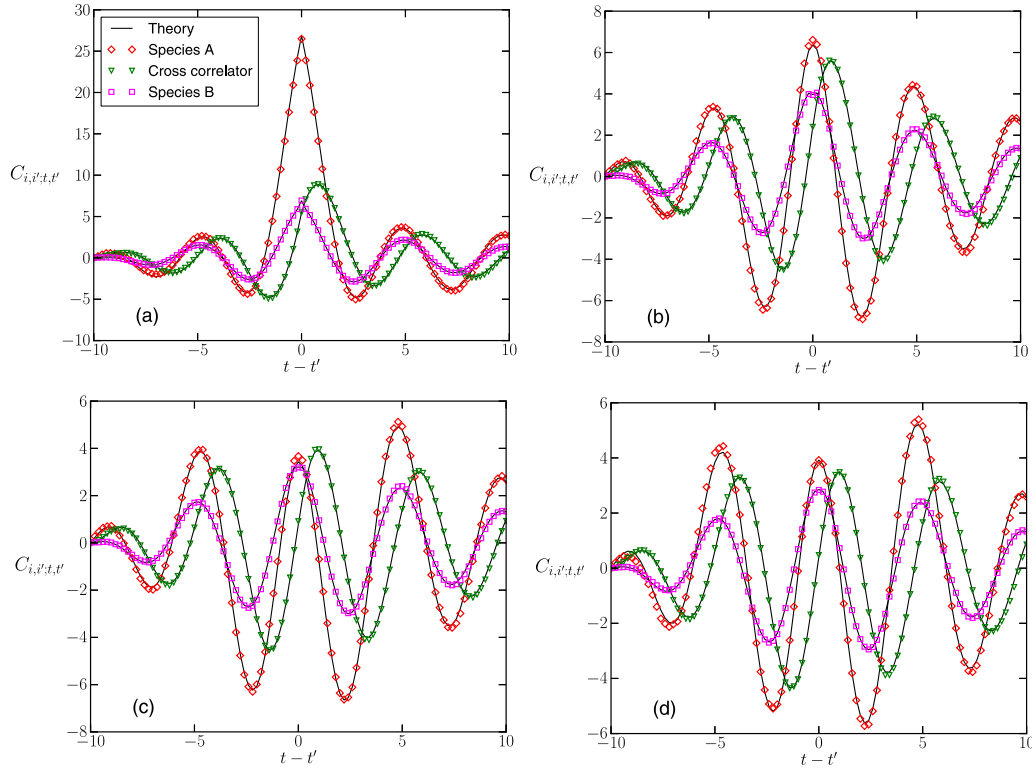
FIG. 2. The correlators $C_{i,i';t,t'} = \frac{\langle \delta^\alpha_{i,t} \delta^{\alpha'}_{i',t'} \rangle}{N}$ for various spatial and temporal separations for the Lengyel-Epstein model with both species subdiffusing. Monte Carlo simulation results are shown as hollow markers and the lines from the theory are solid black. The species A autocorrelator results are red diamonds, the species B autocorrelator results are magenta squares, and the cross-correlator results are green triangles. The model parameters are $a = 5$, $b = 0.7$, $c = 1$, $d = 1$, $t_0^{(1)} = 2.0$, $t_0^{(2)} = 0.05$, $\gamma^{(1)} = 0.5$, and $\gamma^{(2)} = 0.75$. The system-size is $N = 10\,000$ and the number of trials over which the simulations were averaged is 8000. The simulations were performed on a discrete lattice with 7 sites and periodic boundary conditions. The spatial separations are (a) $i - i' = 0$; (b) $i - i' = 1$; (c) $i - i' = 2$; (d) $i - i' = 3$.

To carry out the simulations, it was necessary to modify the Gillespie algorithm [56] in a similar way to Ref. [57]. This was due to the non-Markovian nature of the hopping processes. Broadly, the simulations involve keeping a list of the scheduled hopping times of particles, carrying these out at appropriate times and in the right sequence, while performing reactions in the intermediate times. The full procedure is given in the Appendix. To the best of our knowledge, individual-based simulations of reaction-diffusion systems with subdiffusive transport have not been performed in this way previously.

The full expressions for the correlators $\langle \delta^\alpha_{i,t} \delta^{\alpha'}_{i',t'} \rangle$, from which the theory lines in Figs. 1 and 2 are derived, can be found in Sec. S5 of the Supplemental Material [31]. In the Supplemental Material we also explain how the equal-time correlators in Fig. 1 can be found without the use of a numerical inverse Laplace transform.

VI. ONSET OF STOCHASTIC AND DETERMINISTIC TURING PATTERNS

A. Description of the phenomena

In a deterministic system which exhibits a Turing instability, a finite range of Fourier modes with nonzero wave numbers is unstable. That is to say, if the system is perturbed from its uniform fixed point, then the amplitudes of these modes will grow with time. A criterion for the Turing

instability in systems with one subdiffusing component and one normally diffusing component is given in Refs. [18,19]. In practice, particle numbers do not deviate infinitely far from the fixed point. Instead, the growth of the unstable modes is curtailed by the nonlinearity of the reaction equations. If one simulates systems with such an instability and looks at the Fourier transform of deviations from the uniform state, then one finds the dominant peak at a nonzero wave number. It is this wave number which characterizes the periodicity of the observed Turing patterns. It is important to note that noise is not required to sustain these patterns once the initial perturbation about the uniform state has been applied. In particular, the amplitude of these deterministic patterns is set by the nonlinearities of the reaction-(sub)diffusion system and not by any source of stochasticity.

However, one may also observe patterns in systems with finite particle number (i.e., systems with intrinsic noise), even when the parameters are such that the purely deterministic system would not show any patterns [10,11]. These patterns are noise-driven, and their amplitude is set by the strength of the noise; in individual-based systems the variance of the intrinsic noise in turn is determined by the inverse typical particle number N^{-1}. We refer to patterns formed in this way as quasipatterns or stochastic Turing patterns. They can be detected in the Fourier spectra of fluctuations about the uniform deterministic fixed point; these spectra show a peak at
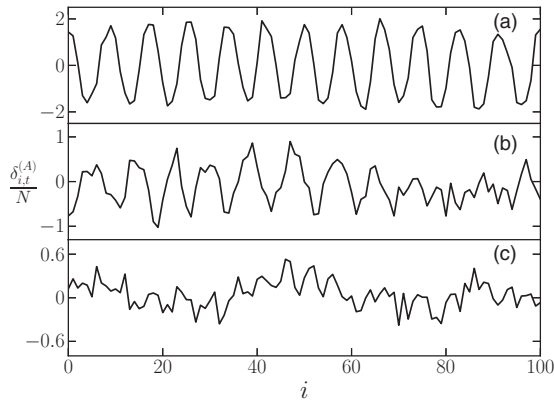
FIG. 3. Comparison of the spatial patterns produced in the Lengyel-Epstein model. (a) Parameters are in the phase where deterministic pattern formation occurs ($t_0^{(A)} = 0.2$, $t_0^{(B)} = 0.1$). (b) Noise-induced patterns but no deterministic patterns ($t_0^{(A)} = 0.11$, $t_0^{(B)} = 0.1$). (c) No patterns are found at all ($t_0^{(A)} = 0.1$, $t_0^{(B)} = 0.2$). In these simulations, $N = 1000$, the activator subdiffuses with $\gamma = 0.5$, the inhibitor diffuses normally. Reaction rates are given in the caption of Fig. 4. The parameter sets used in the three panels correspond to those marked by the three blue dots in Fig. 4.

a characteristic nonzero wave number. In contrast to deterministic Turing patterns, this peak is not observed in the absence of noise. Such patterns have been analyzed in systems with regular diffusion; see, e.g., Refs. [10,11,13,14].

In Fig. 3 we show examples of Turing patterns in the Lenyel-Epstein system with subdiffusion. The data in the upper panel is from individual-based simulations in the parameter regime in which the deterministic model shows Turing patterns. The pattern is seen in the individual-based simulation as well, but it is important to stress that this is not a noise-driven pattern. The stochasticity in the individual-based model modulates the deterministic pattern, but the amplitude of the structure is independent of the noise, i.e., increasing the number of particles, N, per site does not change the relative magnitude of the pattern. In the central panel we show an

example of a quasipattern. This data is taken in the regime in which the deterministic Lengyel-Epstein system does not have any instability; the pattern is purely noise-driven and its amplitude decreases with increasing particle number per lattice site. One further main difference between stochastic and deterministic patterns is that the stochastic patterns are not stationary. Instead, regions of high concentration for one chemical species continually assemble, shift, and dissipate in such a manner that a typical level of periodicity is maintained. Deterministic patterns on the other hand are stationary in time. In the lower panel of Fig. 3, finally, the parameters are such that neither deterministic nor stochastic Turing patterns are seen. The system fluctuates about the deterministic uniform fixed point, but no particular spatial structure emerges in these fluctuations. That being said, the fluctuations do appear to be quite large in magnitude, given the system size. Similarly, the magnitude of the noise-induced pattern in Fig. 3(b) is comparable to that of the pattern in Fig. 3(a). This is not an unusual observation and is due to a phenomenon known as "stochastic amplification," which has been reported in the context of noise-driven cycles and patterns in normally diffusing systems (see, e.g., Refs. [10,11,13,46,58]).

B. Phase diagrams

The theory we developed in the earlier sections allows us to find the equal-time correlator in Fourier space (i.e., the structure factor $\langle \tilde{\delta}_{q,t}^{(\alpha)} \tilde{\delta}_{q,t}^{(\alpha')\star} \rangle$) of fluctuations without having to carry out time-consuming simulations. We can use these expressions to search parameter space and to identify the regimes in which stochastic patterns emerge, and the parameter ranges where they do not. This gives a more complete picture of the effect of subdiffusion on stochastic pattern formation. Our results are summarized in the phase diagrams in Figs. 4 and 5, which we discuss in more detail below. While the expressions from the theory have to be evaluated numerically, we note that determining the phase behavior from the analytical expressions is very efficient; accurately establishing the phase
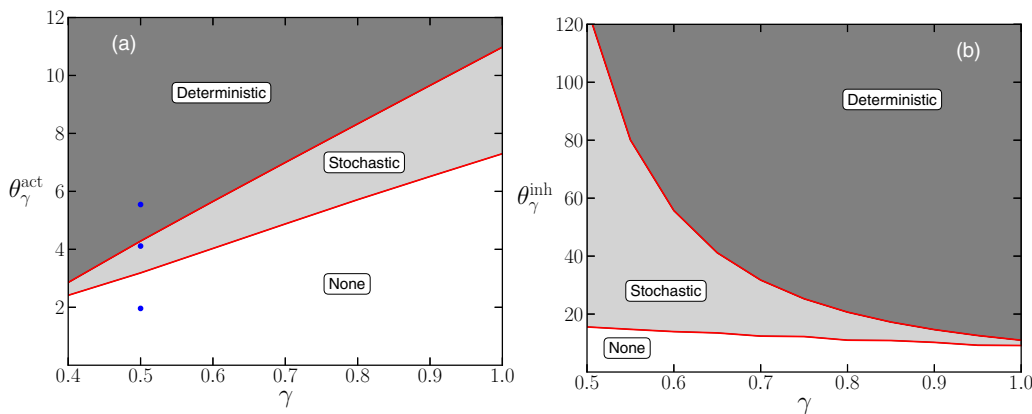

FIG. 4. Phase diagrams showing the parameter regions where deterministic Turing patterns (dark gray shading) and stochastic (noise-driven) patterns (light gray) occur for the Lengyel-Epstein model. Panels (a) and (b) show the behavior when the activator and the inhibitor subdiffuse, respectively. The other component diffuses normally. As γ decreases, and the diffusion becomes more anomalous, the critical values of θ_γ at which deterministic and stochastic patterns emerge decrease for the subdiffusing activator (a) and increase for the subdiffusing inhibitor (b). When $\gamma = 1$, the diffusion is normal and the critical values of θ_γ in both plots are the same. The remaining model parameters are $a = 2$, $b = 0.13$, $c = d = 1$.
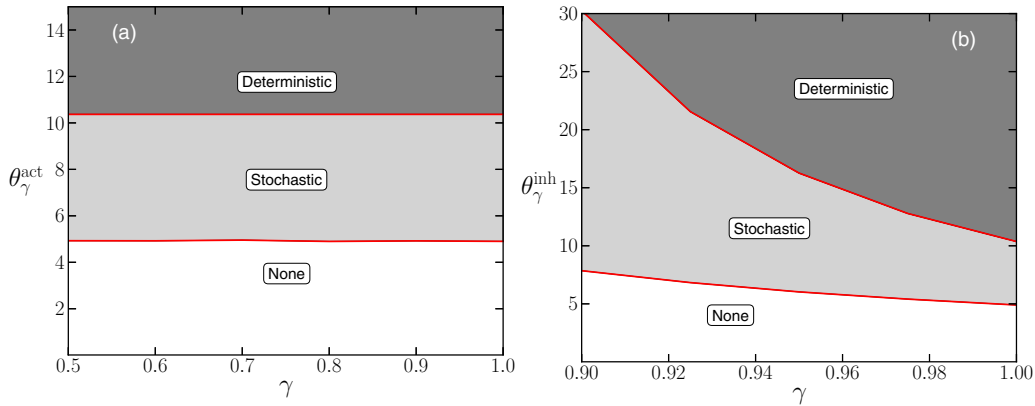
FIG. 5. Phase diagrams showing the parameter regions where deterministic Turing patterns (dark gray shading) and stochastic (noise-driven) patterns (light gray) occur for the Brusselator model. Panels (a) and (b) show the behavior when the activator and the inhibitor subdiffuse, respectively. The other component diffuses normally. Due to the constant death-rate of the activator, the critical value of θ_γ for the onset of both stochastic and deterministic patterns does not vary with γ when the activator subdiffuses (a). When the inhibitor (with concentration-dependent death rate) subdiffuses (b), the behavior is qualitatively similar to that seen in the Lengyel-Epstein model in Fig. 4. When $\gamma = 1$, the diffusion is normal and the critical values of θ_γ in both plots are the same. The remaining model parameters are $a = 1.1$, $b = 1.8$.

diagrams from individual-based simulations, however, would require unrealistic computing time.

It is well-known that the emergence of deterministic Turing patterns relies on the slow diffusion of the activator and the comparatively fast diffusion of the inhibitor. In previous work [19] we showed that it is possible to define effective diffusion coefficients for systems in which one reactant undergoes subdiffusion and the other normal diffusion; see also Ref. [18]. To characterize the degree to which the rates of (sub)diffusion of the two particle species differ, we define the ratio of these effective diffusion constants, θ_γ; see again Refs. [18,19] for details. The detailed definition depends on which one of the components (activator or inhibitor) is subdiffusing. We have

$$\theta_\gamma^{\mathrm{act}} = \frac{\left(t_0^{(\mathrm{act})}\right)^\gamma}{t_0^{(\mathrm{inh})}\left(\bar{p}^{(\mathrm{act})}\right)^{1-\gamma}}, \qquad (19)$$

when the activator subdiffuses, and

$$\theta_\gamma^{\mathrm{inh}} = \frac{t_0^{(\mathrm{act})}\left(\bar{p}^{(\mathrm{inh})}\right)^{1-\gamma}}{\left(t_0^{(\mathrm{inh})}\right)^\gamma}, \qquad (20)$$

when the inhibitor subdiffuses. The quantity $\bar{p}$ in these expressions denotes the per capita removal rate of the relevant substance at the uniform deterministic fixed point.

Figures 4 and 5 show the critical ratios of the effective diffusion constants of the activator and the inhibitor for the onset of stochastic and deterministic Turing patterns in the Lengyel-Epstein and Brusselator models, respectively. For any fixed value of the anomalous exponent γ the following behavior is observed in Figs. 4 and 5. For low values of θ_γ, neither deterministic nor stochastic patterns emerge. As the ratio of effective diffusion coefficients is increased and crosses a first critical threshold, θ_γ^s, a phase is entered in which stochastic patterns are found, but where the deterministic system shows no patterns. As θ_γ is increased further, the system undergoes a full deterministic Turing instability at θ_γ^d.

Additionally, we find that, in general, if the subdiffusion of a particular reactant is conducive to the formation of

deterministic patterns, then it is also conducive to the formation of stochastic patterns. Similarly, if subdiffusion of a reactant makes deterministic pattern formation more difficult, then it also reduces the parameter range in which noise-driven patterns are found. In other words, if the critical value θ_γ^d for the onset deterministic patterns increases (decreases) with γ, then θ_γ^s also increases (decreases) with γ.

One notes that due to the concentration-independent decay rate of the activator in the Brusselator model, both θ_γ^d and θ_γ^s do not vary with the anomalous exponent γ when the activator is subdiffusing (left-hand panel in Fig. 5). However, if the death rate of the subdiffusing component is not constant, then one finds that, in our examples, as γ decreases, so do both θ_γ^d and θ_γ^s if the activator is subdiffusing (left-hand panel of Fig. 4). Conversely, if the inhibitor is subdiffusing and the inhibitor death rate is concentration-dependent, a reduced value of γ makes it more difficult it is for Turing patterns to form (right-hand panels of Figs. 4 and 5).

One caveat to the approach we have presented is that analytical results are only valid for large system sizes N. That being said, the qualitative conclusions we have reached (that the combination of stochasticity and subdiffusion lowers the threshold for pattern formation) can be extended to the regime of moderate N, where the theory is not as accurate. We have verified this in simulations, and discuss this point briefly in Sec. 6 of the Supplemental Material [31].

VII. SUMMARY AND CONCLUSIONS

We have successfully extended the description of reaction-diffusion systems with anomalous transport to include the intrinsic noise which comes about when the number of particles in the system is finite. To do this, we carried out a Gaussian approximation of the individual-based system, using a generating-functional approach. We also provided a prescription for finding the fluctuations about the stable homogeneous fixed point of reaction-diffusion systems with anomalous diffusion. This was done in the example cases

of the Brusselator and Lengyel-Epstein systems, and our theoretical predictions were successfully tested against computer simulations. Finally, we used this theory to determine the parameter regimes where one could expect to observe stochastic Turing patterns. We found examples for which a subdiffusing activator encouraged both stochastic and deterministic pattern formation, whereas a subdiffusing inhibitor hindered both stochastic and deterministic pattern formation. This is exemplified in Figs. 1, 4, and 5.

The theory developed in this paper is entirely general and would be equally applicable to any reaction scheme with anomalously diffusing reactants; the two examples discussed here were mainly chosen for illustration. Systems such as the Lotka-Volterra [59] dynamics, the Oregonator [60–62], or the Schnakenberg model [63] with subdiffusion would have been equally valid candidates for the study of noise-driven patterns. We could also have studied systems with different waiting-time distributions or hopping kernels.

A well-known problem with using Turing's mechanism as an explanation for pattern formation in nature is the often unphysically large ratio of the diffusion constants required for the instability to occur. Both subdiffusion and stochastic pattern formation have been proposed separately as potential remedies for this problem. In this paper, we have shown that a combination of the two can lower the threshold for pattern formation to a greater degree than either mechanism on its own. This is demonstrated by the fact that the critical ratio of the diffusion constants is always lower in Figs. 4 and 5 for the onset of stochastic patterns than it is for deterministic patterns, and by the fact that this critical ratio can reduce as the activator becomes more subdiffusive.

Recently, the existence of noise-induced Turing patterns in bacterial cultures has been examined [14]. However, these experiments were concerned with a mechanism for pattern formation for which the diffusion was presumed to be Markovian. A possibility for further experiment would be to analyze stochastic pattern formation in a system in which the diffusion of the reactants was known to be subdiffusive. Our approach makes predictions for the way in which noise-driven pattern formation is affected by subdiffusion.

Another question for future study would be to ask how other stochastic phenomena in reaction-diffusion systems, such as waves [64], would be affected by anomalous diffusion. Conversely, one might also wonder about how such phenomena are affected by superdiffusion. The theoretical approach we have developed is sufficiently general, and can be applied to the study of such systems.

APPENDIX: INDIVIDUAL-BASED SIMULATIONS

The non-Markovian nature of subdiffusive hopping requires us to modify the traditional Gillespie algorithm [56], in a similar way to Ref. [57]. The statistics of the processes laid out in Sec. II A are preserved by using the following algorithm:

(1) Set $t = 0$ and initialize the system. (In our simulations, we start from $n_i^{(1)} = \bar{n}^{(1)}$ and $n_i^{(2)} = \bar{n}^{(2)}$.) For each particle draw a waiting time until its next hop from the appropriate distribution, and create a list of all scheduled hopping events.

(2) Take note of the earliest hopping time and the position of the particle associated with this time; we label the time at which the next hop occurs $\tau^{(H)}$.

(3) Based on the numbers of particles at each position, calculate the reaction rates for each type of reaction and each point on the lattice, $\lambda_{i,r,t}$. Calculate the sum of the reaction rates $\lambda_t = \sum_{r,i} \lambda_{i,r,t}$ and draw the time at which the next reaction is due to occur: $\tau^{(R)} = t - \frac{1}{\lambda_t} \ln(s)$, where s is an independent random number from the uniform distribution over (0,1]. This reaction can occur at any position on the lattice.

(4) (a) If $\tau^{(R)} < \tau^{(H)}$, then perform one single reaction. Choose this to be a reaction of type r at site i with probability $\lambda_{i,r,t}/\lambda_t$. If particles are removed during this reaction, then delete the scheduled hopping events for these particles from the list. If particles are created, then draw hopping times from the appropriate distribution, and add these to the list of scheduled hops. Set $t = \tau^{(R)}$. Go to 2.

(b) If $\tau^{(R)} > \tau^{(H)}$, then perform the hop associated with $\tau^{(H)}$ in step 2, and discard the reaction event from step 3. To do this draw a random hopping distance from the hopping kernel $\phi_{i,i'}$, and relocate the particle. Draw a new waiting time until the next hop of this particle, and add this time to the list. Set $t = \tau^{(H)}$. Go to 2.

To draw waiting times from the Mittag-Leffler distribution in Eq. (5), one can use the following formula $t = -t_0^\alpha \ln(u) \left(\frac{\sin(\gamma^\alpha \pi)}{\tan(\gamma^\alpha \pi v)} - \cos(\gamma^\alpha \pi) \right)^{\frac{1}{\gamma^\alpha}}$ [65,66], where u and v are independent random numbers from a uniform distribution on (0,1].

[1] A. Gierer and H. Meinhardt, Kybernetik **12**, 30 (1972).

[2] J. Murray, Phil. Trans. R. Soc. Lond. B **295**, 473 (1981).

[3] J. Murray, J. Theor. Biol. **88**, 161 (1981).

[4] V. Petrov, Q. Ouyang, and H. L. Swinney, Nature **388**, 655 (1997).

[5] M. Falcke and H. Levine, Phys. Rev. Lett. **80**, 3875 (1998).

[6] J. Van de Koppel, J. C. Gascoigne, G. Theraulaz, M. Rietkerk, W. M. Mooij, and P. M. Herman, Science **322**, 739 (2008).

[7] J. Rayleigh, Philos. Mag. **32**, 529 (1916).

[8] A. M. Turing, Philos. Trans. Royal Soc. B **237**, 37 (1952).

[9] J. Murray, *Mathematical Biology*, 3rd ed. (Springer, New York, 2004).

[10] T. Butler and N. Goldenfeld, Phys. Rev. E **80**, 030902(R) (2009).

[11] T. Butler and N. Goldenfeld, Phys. Rev. E **84**, 011112 (2011).

[12] T. Biancalani, F. Jafarpour, and N. Goldenfeld, Phys. Rev. Lett. **118**, 018101 (2017).

[13] T. Biancalani, D. Fanelli, and F. Di Patti, Phys. Rev. E **81**, 046215 (2010).

[14] D. Karig, K. M. Martini, T. Lu, N. A. DeLateur, N. Goldenfeld, and R. Weiss, Proc. Natl. Acad. Sci. USA **115**, 6572 (2018).

[15] F. Di Patti, L. Lavacchi, R. Arbel-Goren, L. Schein-Lubomirsky, D. Fanelli, and J. Stavans, PLoS Biol. **16**, 1 (2018).

[16] R. Metzler and J. Klafter, Phys. Rep. **339**, 1 (2000).

[17] R. Metzler and J. Klafter, J. Phys. A **37**, R161 (2004).

[18] A. Yadav, S. M. Milu, and W. Horsthemke, Phys. Rev. E **78**, 026116 (2008).

[19] J. W. Baron and T. Galla, Phys. Rev. E **99**, 012212 (2019).

[20] R. Ghosh and W. Webb, Biophys. J. **66**, 1301 (1994).

[21] P. Schwille, J. Korlach, and W. W. Webb, Cytometry **36**, 176 (1999).

[22] M. J. Saxton, Biophys. J. **67**, 2110 (1994).

[23] M. J. Saxton, Biophys. J. **70**, 1250 (1996).

[24] G. Hornung, B. Berkowitz, and N. Barkai, Phys. Rev. E **72**, 041916 (2005).

[25] S. B. Yuste, E. Abad, and K. Lindenberg, Phys. Rev. E **82**, 061123 (2010).

[26] S. Fedotov and S. Falconer, Phys. Rev. E **89**, 012107 (2014).

[27] S. Fedotov and S. Falconer, Phys. Rev. E **87**, 052139 (2013).

[28] P. Glansdorff and I. Prigogine, *Thermodynamic Theory of Structure, Stability and Fluctuations* (Wiley-Interscience, New York, 1971).

[29] I. Lengyel, G. Rabai, and I. R. Epstein, J. Am. Chem. Soc. **112**, 9104 (1990).

[30] I. Lengyel and I. R. Epstein, Science **251**, 650 (1991).

[31] See Supplemental Material at http://link.aps.org/supplemental/10.1103/PhysRevE.99.052124 for further details of the calculations discussed in the main text.

[32] A. McNaught and A. Wilkinson, *Compendium of Chemical Terminology* (Blackwell Science, Oxford, 1997), Vol. 1669.

[33] F. Mainardi and R. Gorenflo, J. Comput. Appl. Math. **118**, 283 (2000).

[34] M. F. Shlesinger, Eur. Phys. J. B **90**, 93 (2017).

[35] E. W. Montroll and G. H. Weiss, J. Math. Phys. **6**, 167 (1965).

[36] R. Klages, G. Radons, and I. M. Sokolov, *Anomalous Transport: Foundations and Applications* (Wiley-VCH, Weinheim, 2008).

[37] V. Mendez, S. Fedotov, and W. Horsthemke, *Reaction-transport Systems: Mesoscopic Foundations, Fronts, and Spatial Instabilities* (Springer, New York, 2010).

[38] J. J. Tyson, *The Belousov-Zhabotinskii Reaction* (Springer-Verlag, Berlin Heidelberg, 1976).

[39] V. Castets, E. Dulos, J. Boissonade, and P. De Kepper, Phys. Rev. Lett. **64**, 2953 (1990).

[40] P. Érdi and J. Tóth, *Mathematical Models of Chemical Reactions: Theory and Applications of Deterministic and Stochastic Models* (Manchester University Press, Manchester, 1989).

[41] N. G. Van Kampen, *Stochastic Processes in Physics and Chemistry* (Elsevier, London, 1992), Vol. 1.

[42] C. W. Gardiner, *Handbook of Stochastic Methods for Physics, Chemistry, and the Natural Sciences*, 4th ed. (Springer, New York, 2009).

[43] D. R. Cox, *The Theory of Stochastic Processes* (Routledge, London, 2017).

[44] D. T. Gillespie, J. Chem. Phys. **115**, 1716 (2001).

[45] H. Risken, *The Fokker-Planck Equation* (Springer, New York, 1996).

[46] A. J. McKane and T. J. Newman, Phys. Rev. Lett. **94**, 218102 (2005).

[47] P. C. Martin, E. D. Siggia, and H. A. Rose, Phys. Rev. A **8**, 423 (1973).

[48] H.-K. Janssen, Z. Phys. B **23**, 377 (1976).

[49] C. De Dominicis, J. Phys. Colloques **37**, C1-247 (1976).

[50] T. Brett and T. Galla, Phys. Rev. Lett. **110**, 250601 (2013).

[51] T. Brett and T. Galla, J. Chem. Phys. **140**, 124112 (2014).

[52] A. Altland and B. D. Simons, *Condensed Matter Field Theory* (Cambridge University Press, Cambridge, 2010).

[53] M. O. Vlad and J. Ross, Phys. Rev. E **66**, 061908 (2002).

[54] S. Fedotov and S. Falconer, Phys. Rev. E **85**, 031132 (2012).

[55] D. Halsted and D. Brown, Chem. Eng. J. **3**, 312 (1972).

[56] D. T. Gillespie, J. Comput. Phys. **22**, 403 (1976).

[57] D. F. Anderson, J. Chem. Phys. **127**, 214107 (2007).

[58] D. Alonso, A. J. McKane, and M. Pascual, J. Roy. Soc. Interface **4**, 575 (2007).

[59] A. J. Lotka, J. Phys. Chem. **14**, 271 (1909).

[60] R. J. Field and R. M. Noyes, J. Chem. Phys. **60**, 1877 (1974).

[61] J. J. Tyson and P. C. Fife, J. Chem. Phys. **73**, 2224 (1980).

[62] W. Jahnke, W. E. Skaggs, and A. T. Winfree, J. Phys. Chem. **93**, 740 (1989).

[63] J. Schnakenberg, J. Theor. Biol. **81**, 389 (1979).

[64] T. Biancalani, T. Galla, and A. J. McKane, Phys. Rev. E **84**, 026201 (2011).

[65] D. Fulger, E. Scalas, and G. Germano, Phys. Rev. E **77**, 021122 (2008).

[66] T. J. Kozubowski, J. Comput. Appl. Math. **116**, 221 (2000).